PRAMANA
journal of
physics

© Printed in India

Supplement to Vol. 45
October 1995
pp. 33-46

Limits on 3 boson vertex parameters from LEP200

S. BANERJEE
Tata Institute of Fundamental Research, Bombay 400 005

Abstract. LEP will be operating at cm energies above W pair threshold from 1996. The process $e^+e^- \rightarrow W^+W^-$ will provide a unique opportunity to test some important aspects of the Standard Model. The methodology of studying this process has been reviewed in this report. The study of the process will probe at the triple vector boson coupling. The sensitivity to anomalous coupling of W boson has been discussed in detail.

1. Introduction

One of the main motivations of LEP200 is a study of the process $e^+e^- \rightarrow W^+W^-$. The reaction $e^+e^- \rightarrow W^+W^-$ has contributions from ν exchange in the t-channel and γ, Z exchange in the s-channel. Of these, the ν exchange gives the largest contribution to the amplitude. In the Standard Model [1] large cancellation takes place between the various amplitudes and the resultant cross section is small and well behaved (see figure 1) at high energies. As a result, small deviation from the Standard Model will show up in this process and can be studied at LEP200. The physics possibilities and limitation have been studied in several earlier reviews [2, 3] and some of those results will be highlighted here.

The main importance of studying the process $e^+e^- \rightarrow W^+W^-$ lies in the γWW and ZWW couplings (see figure 2).

The interaction vertex is given by $ig_{WWV}\Gamma_V^{\alpha\beta\mu}(q, \bar{q}, p)$, where V is the vector boson γ or Z.

$$g_{WW\gamma} = -e; \qquad g_{WWZ} = -e\cot\theta_W$$

$\Gamma_V^{\alpha\beta\mu}$ involves 2×7 independent form factors f_i^γ and f_i^Z. The three form factors f_1^V, f_2^V, f_3^V are related to magnetic and electric dipole moments of W. One can write

$$\begin{aligned} f_1^V &= 1 + \frac{s}{2m_W{}^2} \\ f_2^V &= \lambda_V \\ f_3^V &= 1 + \kappa_V + \lambda_V \\ \mu_W &= \frac{e\,(1 + \kappa_\gamma + \lambda_\gamma)}{2m_W} \\ Q_W &= \frac{e\,(\kappa_\gamma - \lambda_\gamma)}{m_W{}^2} \end{aligned}$$

The other form factors are restricted by C, P and CP invariance

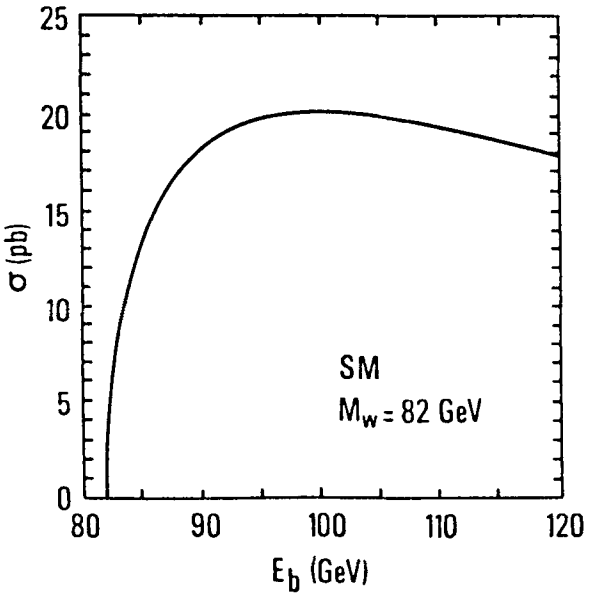

Figure 1. Total cross section for $e^+e^- \rightarrow W^+W^-$ in the Standard Model as a function of beam energy for $m_W = 82$ GeV

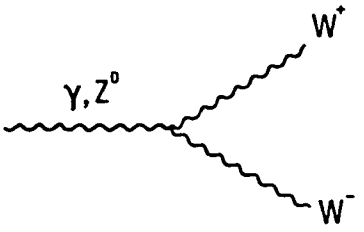

Figure 2. The three boson coupling $Z(\gamma)WW$

$$\begin{array}{lll} \text{CP invaraince} & \Longrightarrow & f_4^V = f_6^V = f_7^V = 0 \\ \text{C and P invariance} & \Longrightarrow & f_4^\gamma = f_5^\gamma = f_6^\gamma = f_7^\gamma = 0 \end{array}$$

In the Standard Model, one has at the lowest order

$$\begin{aligned} \kappa_\gamma &= \kappa_Z = 1 \\ \lambda_\gamma &= \lambda_Z = 0 \\ f_{4,5,6,7}^{\gamma,Z} &= 0 \end{aligned}$$

So to test the validity of the Standard Model, one needs to measure

κ_γ, κ_Z
λ_γ, λ_Z
g_{WWZ}
$f_{4,5,6,7}^Z$

In the various study groups [4], the following parameters have been studied : δg_{WWZ}, λ (with $\lambda_\gamma = \lambda_Z$), κ_γ and κ_Z.

2. Observables

Experimentally, one can make the following measurements :

- Total cross section
- Production angle of W^+ (W^-)
- Decay angular distribution of W^+ and W^-

As seen in figure 1, the W pair cross section is rather small ($\sim$ 20 pb) compared to typical LEP100 cross sections. It is approximately flat over the energy range of interest (at cm energies above 175 GeV). One can expect to observe about 4000 events per year in one experiment if the LEP luminosity reaches 2×10^{31} cm^{-2}sec^{-1}.

In the standard Model, the W couples universally to quarks and leptons. One can write down [2]

$$\Gamma_W = \Gamma(W \to \ell\nu)\left[3 + \left(2 + (1 + \frac{m_t{}^2}{2m_W{}^2})(1 - \frac{m_t{}^4}{m_W{}^4})^2\right)(1 + \frac{\alpha_s}{\pi})\right]$$

This leads to 8.9% of W's decaying to each of the leptonic channels ($e\nu$, $\mu\nu$ or $\tau\nu$) and the remaining 73.3% decaying to $q\bar{q}'$ system ($u\bar{d}$ or $c\bar{s}$). As a result, out of all the W^+W^- events, one will have the following final states

54%	4 jets (pure hadronic)
39%	$j_1\, j_2\, \ell\, \nu$ (semi leptonic)
7%	$\ell_1\, \nu_1\, \ell_2\, \nu_2$ (pure leptonic)

For the semileptonic final state (j_1 j_2 ℓ ν), one can make the following observations

- j_1 j_2 will determine the folded direction of W

- ℓ determines the charge of W unambiguously. So one can study production angle of W^+ (W^-).
- One can study the complete decay angular distribution of the W which decays leptonically
- One can also study folded decay angular distribution of the W decaying hadronically. If tagging of the jet charge is possible, a study of complete decay angular distribution from W decay can be done.

For pure hadronic final states (j_1 j_2 j_3 j_4), the jets determine W direction. However, one needs some measure of jet charge to decide about the charge of W. So in principle, one can always study folded production angle of W^+ (W^-). Similarly, one can study the folded decay angular distribution of W's.

For pure leptonic final states (ℓ_1 ν_1 ℓ_2 ν_2), the momenta of the two ν's can be calculated within a twofold ambiguity if W width and photons from initial state radiation are ignored. It is nevertheless a very clean sample. But it is difficult to obtain the production or decay angular distribution uniquely.

Production of transversely polarized W ($\lambda = \pm 1$) dominates over that of longitudinally polarized W ($\lambda = 0$) for all values of production angle. However, in the backward region, the dominant $\Delta\lambda = -2$ amplitude from ν exchange vanishes. So this region is more sensitive in measuring the gauge couplings. Decay angular distribution of W depends on W polarization. So a study of the decay distribution helps in separating contributions from different W helicity components.

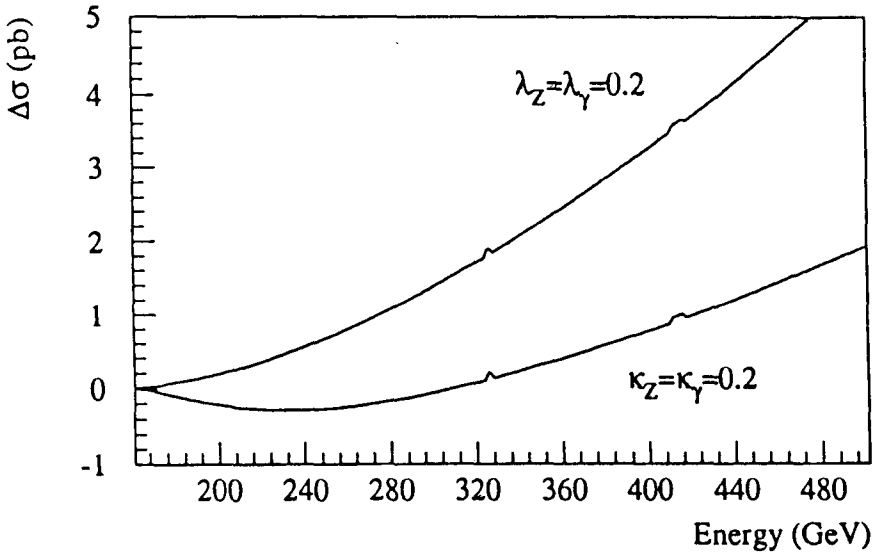

Figure 3. Difference between the SM and non-SM total cross section for $e^+e^- \rightarrow W^+W^-$ as a function of cm energy [4]

Figure 3 shows a plot of deviation of total cross section of $e^+e^- \rightarrow W^+W^-$ from Standard Model value as a function of cm energy for two sets of anomalous 3 boson coupling ($\kappa_\gamma = \kappa_Z = 0.2$ and $\lambda_\gamma = \lambda_Z = 0.2$). The figure clearly shows that large deviation from the Standard Model is seen only at very high cm energy.

So LEP200 operating near the W^+W^- threshold will not be able to detect any significant deviation from the Standard Model from this measurement.

Figure 4 shows distribution of production angle of the W's as expected in the Standard Model and also for some non-standard couplings of the 3 boson system. One sees large deviation from the Standard Model only in the very backward directions. So to be sensitive to anomalous W couplings, the detectors should have a large angular acceptance and also high precision in the forward backward direction.

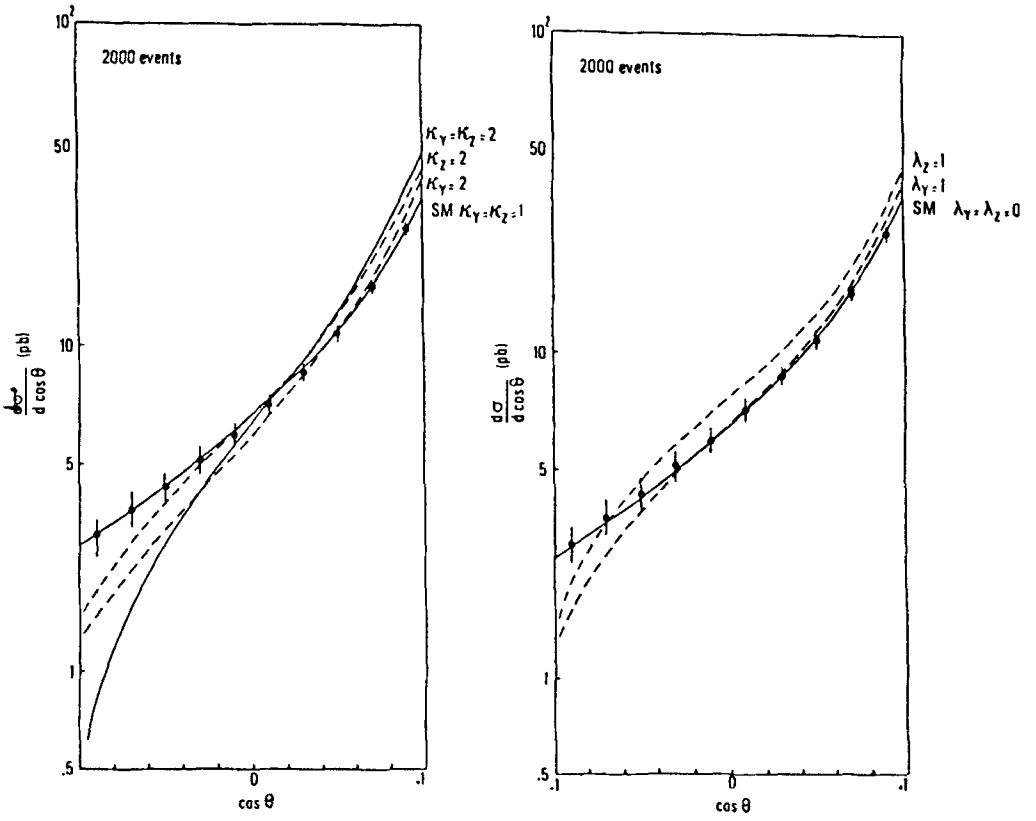

Figure 4. Effect of the angular distribution for W-production due to different values of the parameters κ_γ, κ_Z, λ_γ, λ_Z [3]

3. Event Classification and W Reconstruction

It is necessary to classify the W pair events into three different categories (1) four jet events (j_1 j_2 j_3 j_4); (2) two jet plus two lepton events (j_1 j_2 ℓ ν) and (3) four lepton events (ℓ_1 ν_1 ℓ_2 ν_2) from the general event characteristics and to select these events from a background of other physics events and noise. A first attempt in this direction has been carried out in [5] by looking into fully simulated and reconstructed events from W-pair generator GENTLE [6].

Leptonic decays of W give rise to events with low multiplicity and sizeable missing energy.On the other hand, hadronic decays of W lead to high multiplicity

events with small missing energy. So global event shape variables like visible energy, energy imbalance, total multiplicity would be useful variables for event classification alongwith particle identification capabilities.

Four jet events are classified by selecting events with high multiplicity ($N > 45$), large visible energy ($E_{vis}/\sqrt{s} > 0.72$), small energy imbalance in the transverse direction ($E_\perp/E_{vis} < 0.25$). Leptonic decays of W to $e\nu$ or $\mu\nu$ are removed by rejecting events with electron candidates with energy above 30 GeV or with muon candidates with momentum above 20 GeV. This set of criteria leads to an efficiency of (94±1)% with (98.9±0.5)% purity.

Four lepton events are classified by selecting events with low multiplicity ($N < 12$) and the presence of two high energy leptons (electrons or muons). High energy electrons are selected with energy above 25 GeV and muons with momentum above 20 GeV. The selection efficiency and purity for the three channels $e\nu e\nu$, $\mu\nu\mu\nu$, $e\nu\mu\nu$ as obtained in [5] are summarized in table 1.

Table 1. Selection efficiency and purity of the four lepton final state

	Efficiency	Purity
$e\nu e\nu$	(79±11)%	(92±8)%
$\mu\nu\mu\nu$	(95±5)%	(95±5)%
$e\nu\mu\nu$	(62±13)%	(83±15)%

For events with 2 jets and 2 leptons, one uses the following criteria : (1) moderate multiplicity ($12 < N < 60$), (2) large missing energy ($E_\perp/E_{vis} > 0.1$–0.15), (3) moderate visible energy ($E_{vis}/\sqrt{s} < 0.88$). In addition, separate selection criteria (on energy of identified particles) were applied to classify these into electron, muon or tau category. The resulting efficiency and purity of the samples are summarized in table 2.

Table 2. Selection efficiency and purity of $j_1\, j_2\, \ell\, \nu$ final state

	Efficiency	Purity
$j_1j_2e\nu$	(74±4)%	(87±3)%
$j_1j_2\mu\nu$	(69±4)%	(94±2)%
$j_1j_2\tau\nu$	(80±3)%	(60±3)%

The stable leptons/hadrons are detected in the detector. For W's decaying hadronically, one needs to reconstruct jets. For both W's decaying hadronically, the number of jets to be reconstructed is 4. For only one W decaying hadronically, the number of jets to be reconstructed is 2 (excluding the lepton when associated with e/μ) or 3 (including the lepton when associated with τ). Several jet reconstruction algorithms [7, 8] have been tried out [9]. In most of these algorithms

(JADE, Durham, Geneva and Lund), particles with the smallest closeness variable are combined into clusters until only four clusters are left. The difference in these algorithms lie in the choice of the closeness variable y_{ij} as summarized in table 3.

Table 3. Closeness variable y_{ij} for various jet algorithms

Algorithm	y_{ij}
JADE	$2E_iE_j(1-\cos\theta_{ij})/{E_{vis}}^2$
Durham	$2\mathrm{Min}(E_i^2,E_j^2)(1-\cos\theta_{ij})/{E_{vis}}^2$
Geneva	$8E_iE_j(1-\cos\theta_{ij})/9(E_i+E_j)^2$
Lund	$2\lvert\vec{p}_i\rvert\lvert\vec{p}_j\rvert\sin(\theta_{ij}/2)/\lvert\vec{p}_i+\vec{p}_j\rvert$

In generalized thrust approach [8], one defines the generalized thrust as

$$T_4 = \max_{\vec{n}_j}\left(\frac{\sum_i \max_j(\vec{p}_i\cdot\vec{n}_j)}{\sum_i|\vec{p}_i|}\right)$$

by dividing the set of particles into 4 groups. T_4 is maximized by regrouping particles and finding the four jet axes from the particle 4-momenta in each group. Technically this is achieved by

- Defining event plane according to the 2 largest eigenvectors of the momentum tensor
- Maximizing T_3 on the event plane by dividing the particles in zones of ϕ angle
- Removing the nicest of the three jets (one with the largest thrust)
- Boosting the rest of the particles in the reduced cm system
- Applying the same 3 jet algorithm to divide these particles to a set of 3 jets
- Checking if the particles in each of the jet has the largest $p_{\parallel}$ with respect to the jet. If not, reclassification is required.

Jet energies are recalculated using the jet angles as measured, assuming 0 parton mass and energy momentum conservation.

The energy and angular resolution of the jets, thus obtained, are summarized in table 4.

This study suggests that Durham or Lund algorithm is most suitable for jet reconstruction.

Further constraint can be put by imposing energy-momentum conservation in the W-pair production process. These conservation relations as well as the mass shell criteria for the W's can be written down as

$$(p_{j_1}+p_{j_2}+p_3+p_4\,(+p_\gamma))-\begin{pmatrix}\sqrt{s}\\0\\0\\0\end{pmatrix}=f_{1\cdots4}$$

Table 4. Energy and angular resolution of jets obtained in different jet algorithms

Reconstruction method	σ_E (GeV)	σ_θ (rad)	σ_ϕi (rad)
JADE	6.13	0.113	0.121
Durham	5.96	0.110	0.118
Geneva	6.16	0.115	0.126
Lund	5.58	0.107	0.115
Generalized Thrust	8.50	0.143	0.145

$$(p_{j_1} + p_{j_2})^2 - m^2_{W_1} = f_5$$
$$(p_3 + p_4)^2 - m^2_{W_2} = f_6$$

$p_3 \equiv p_{j_3}$, $p_4 \equiv p_{j_4}$ for four jet final states and $p_3 \equiv p_\ell$, $p_4 \equiv p_\nu$ for $j_1 j_2 \ell\nu$ final state. For perfect measurements, one should have

$$f_j = 0$$

However, because of detector resolution and acceptance, the constraint relations are strictly speaking not satisfied. Energy and direction of the jets and the charged leptons are measured with precision determined by detector resolution and acceptance. After m_W, Γ_W measurement, m_{W_1}, m_{W_2} would be known with some precision. For $j_1\ j_2\ \ell\nu$ final state, $\vec{p}_\nu$ is unmeasured. All these are taken care of by using the method of Lagrangian multiplier. Here one minimizes χ^2 of deviation of measured quatities in an iterative way.

$$\chi^2 = \sum_i \frac{(x_i - x_i^f)^2}{\sigma_i^2} + \sum_j \xi_j f_j$$

The minimum χ^2 should occur for $f_j = 0$ so that the choice of multipliers ξ_j is arbitary. Convergence of the fits are decided by

- the maximum constraint value after fit (e.g. $|f_j| < 10$)
- χ^2 to be small after fit and change of χ^2 in iteration to be also small

The effect of the kinematic fit [10] is summarized in table 5 and figure 5 where one shows the resolutions in production and decay angles of the W's before and after the fit.
The fit improves resolution in all measured distributions.

DELPHI [4] has proposed to use momentum weighted charge of the decay products to measure the charge of the W.

$$C = \sum_i Q_i p_i^\alpha$$

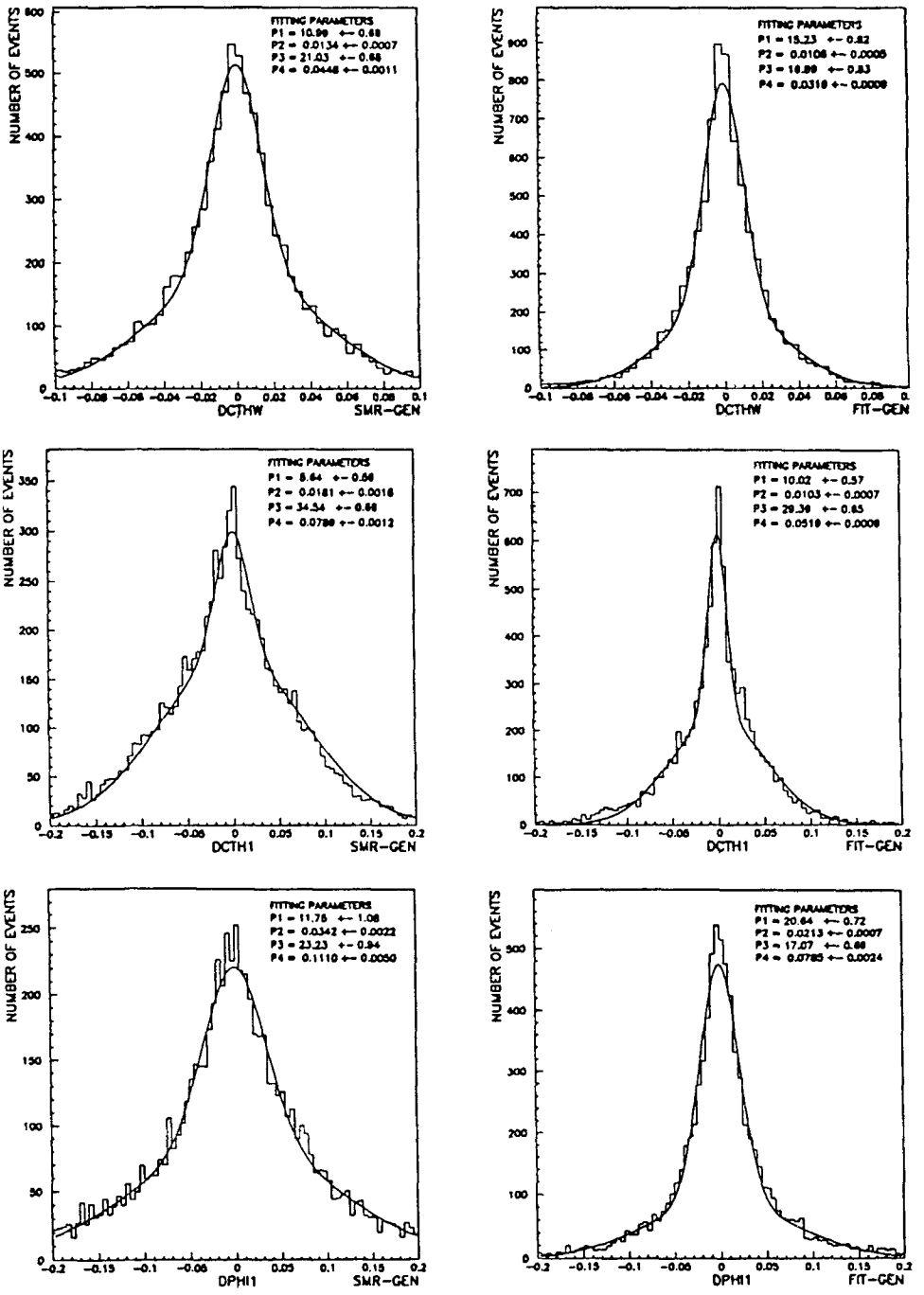

Figure 5. Production (a-b) and decay θ (c-d), ϕ (e-f) angular distribution of W before and after the kinematic fits

Table 5. Resolution in production and decay angular distribution of W before and after the kinematic fit

	Before fit	After fit
$\cos\theta_W$	0.0134	0.0108
$\cos\theta_d$	0.0181	0.0103
ϕ_d (rad)	0.034	0.021

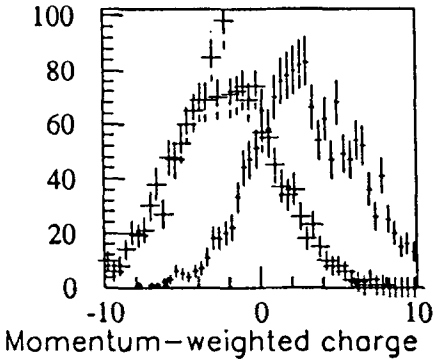

Figure 6. Distribution of momentum weighted charges C_- (the left one) and C_+ (the right one) for jets assigned to W^- and W^+ respectively

where Q and p are charge and momentum of each track assigned to the jets forming W. W^+ and W^- have well separated C parameter value as shown in figure 6. One can use a cut of $|\Delta C| \geq 3$ and choose the W with smaller C value to be W^-. This determines the W charge in the 4 jet sample. There is some misassignment of W charge resulting in a spurious backward peak. However, the cut on C parameter removes $\sim$ 30% of the events.

4. Determination of the 3 Boson Couplings

DELPHI [4] has studied the limits which can be realistically set to the parameters of the 3 boson coupling by their detector. They have generated events with complete detector simulation. After the jet reconstruction and kinematic fitting, they correct the observed W production angular distribution from detector effects by deconvoluting the observed distribution with a binned smearing matrix $F(\cos\theta_W^{cor}, \cos\theta_W^{ob})$

$$\frac{d\sigma}{d\cos\theta_W^{cor}} = \int_{-1}^{1} \frac{d\sigma}{d\cos\theta_W^{ob}} \cdot F(\cos\theta_W^{cor}, \cos\theta_W^{ob}) \cdot \epsilon(\cos\theta_W^{ob}) \cdot d\cos\theta_W^{ob}$$

where $\epsilon(\cos\theta_W^{ob})$ represents the efficiency of the selection criteria for the appropriate final state. For 4 jet final states, they apply the jet charge tagging technique to distinguish between W^+ and W^-.

The corrected distribution is then fitted to the theory by varying each of the parameters (δg_{WWZ}, λ, κ_γ and κ_Z) in turn for 500 pb^{-1} data. The results obtained for two cm energies of 176 and 190 GeV are summarized in table 6.

Table 6. Precision in measuring anomalous 3 boson coupling constant for single parameter fit

	$\sqrt{s} = 176$ GeV	$\sqrt{s} = 190$ GeV
δg_{WWZ}	0.051 ± 0.151	-0.166 ± 0.085
λ	0.034 ± 0.095	-0.095 ± 0.048
κ_γ	1.07 ± 0.20	0.86 ± 0.09
κ_Z	1.05 ± 0.16	0.85 ± 0.08

Thus the anomalous coupling can be measured with a precision of 0.1–0.2 for LEP200 operating at a cm energy of 176 GeV. The precision is improved by a factor of 2 by going to a higher cm energy of 190 GeV.

Alternately, one can fit to several parameters simultaneously. This will give rise to contours at 95% confidence level. Figure 7 shows such contours for δg_{WWZ} vs λ for a two parameter fit to generated and reconstructed angular distributions from $j_1 j_2 \ell\nu$ events.

One can draw the following conclusions from these fits

- The constraint on λ is tight and is not too dependent on the values of other parameters

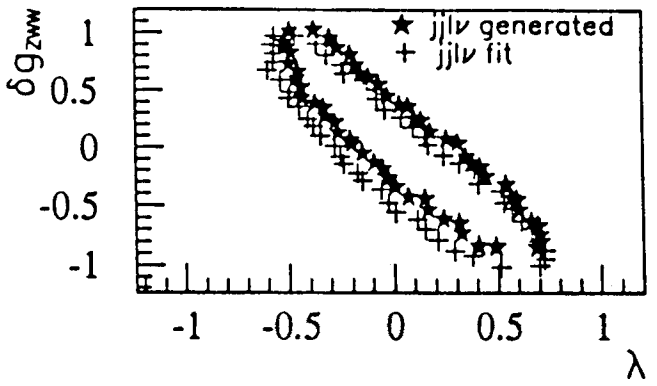

Figure 7. 95% Confidence level contour obtained for δg_{WWZ} and λ from generated and reconstructed production angular distributions using $j_1 j_2 \ell\nu$ events [4]

- The jet charge tagging improves the limits significantly
- One obtains better precision for the anomalous couplings by going to higher cm energies

As has been mentioned earlier, decay angles can be unambiguously determined for leptonic decay of W's in $j_1 j_2 \ell\nu$ event sample. For 4 jet final state, one can obtain folded distribution of decay angular distributions. The charge tagging technique does not work very well for individual jets. Following the suggestions of Hagiwara *et al.* [2], one can parametrize the triple differential cross section in terms of a complete set of known orthogonal functions L_i's, which are used to produce projections $F_i^{\pm}$ of the W^+ and W^- production cross sections respectively.

$$\frac{d\sigma(W^{\pm} \to \ell\nu)}{d\cos\theta_W d\cos\theta_d d\phi_d} = \sum_{i=1}^{9} F_i^{\pm}(\cos\theta_W) L_i(\theta_d, \phi_d)$$

One can now examine a set of linear combinations of F_i^+ and F_i^- to put limits to nonstandard 3 boson parameters. DELPHI [4] have examined the effect of including the decay angular distributions to the parameters (see figure 8).
It is obvious from the figure that the decay angular distributions improve the limit on δg_{WWZ} or κ substantially. The parameter space is more restricted at higher cm energies.

5. Summary

From the studies made so far, one can draw the follwing conclusions :

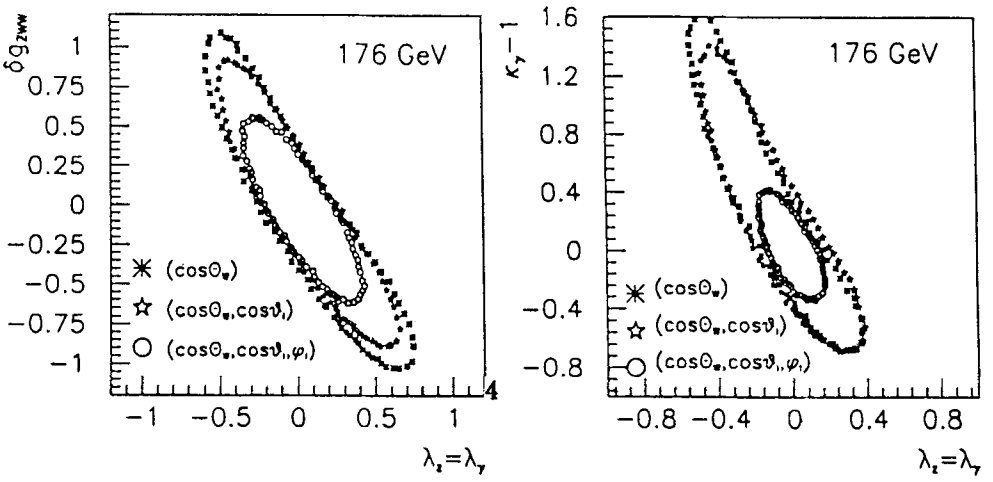

Figure 8. 95% Confidence level contours from the distributions of $\cos\theta_W$, ($\cos\theta_W$, $\cos\theta_d$) and ($\cos\theta_W$, $\cos\theta_d$, ϕ_d) using $j_1j_2\ell\nu$ events [4]

- Techniques have been developed to reconstruct W production and decay angular distributions from the $j_1j_2\ell\nu$ channel as well as the $j_1j_2j_3j_4$ channel. The use of 4 jet channel has the potential of increasing statistics and hence reducing statistical error.
- With 500 pb^{-1} integrated luminosity at LEP200, the 3 boson coupling parameters can be measured from W production angle with a precision of $\pm$0.1-0.2 at 176 GeV.
- Precision of the coupling paramter determination is significantly improved by utilizing the decay angular distribution of W.
- The precision is further improved by operating at a higher energy. Event selection efficiency as well as angular resolution improves with LEP energy.

References

[1] S.L. Glashow, Nucl. Phys. **22** (1961) 579;
S. Weinberg, Phys. Rev. Lett. **19** (1967) 1264;
A. Salam, "Elementary Particle Theory", Ed. N. Svartholm, Stockholm, "Almquist and Wiksell" (1968), 367.

[2] G. Barbiellini *et al.*, in Physics at LEP, ed. J. Ellis and R. Pecci, CERN 86-02, Vol. 2, 1;
K. Hagiwara *et al.*, Nucl. Phys. **B282** (1987) 253.

[3] A. Blondel *et al.*, in ECFA Workshop on LEP200, ed. A. Böhm and W. Hoogland, CERN 87-08, Vol. 1, 120.

[4] S. Katsanevas *et al.*, DELPHI 92-166 Phys 250 (1992).

[5] F. Cavallari and M. Grünewald, L3 Note 1498 (1993).

[6] D. Bardin *et al.*, Phys. Lett. **B308** (1993) 403.

[7] JADE Collaboration, W.Bartel et al., Z. Phys. **C33** (1986) 23;
Y. Dokshizer, J. Phys. **G17** (1991) 1441;
S. Bethke *et al.*, Nucl. Phys. **B370** (1992) 310;
T. Sjostrand, Comp. Phys. Comm. **28** (1983) 227.

[8] S.L. Wu, Z. Phys. **C9** (1981) 329.

[9] T. Aziz *et al.*, L3 Note 1474 (1993).

[10] B.N. Jin and M. Pohl, L3 Note 1479 (1993).